eLIFE
elifesciences.org

Figures and figure supplements

A virus responds instantly to the presence of the vector on the host and forms transmission morphs

Alexandre Martinière, et al.

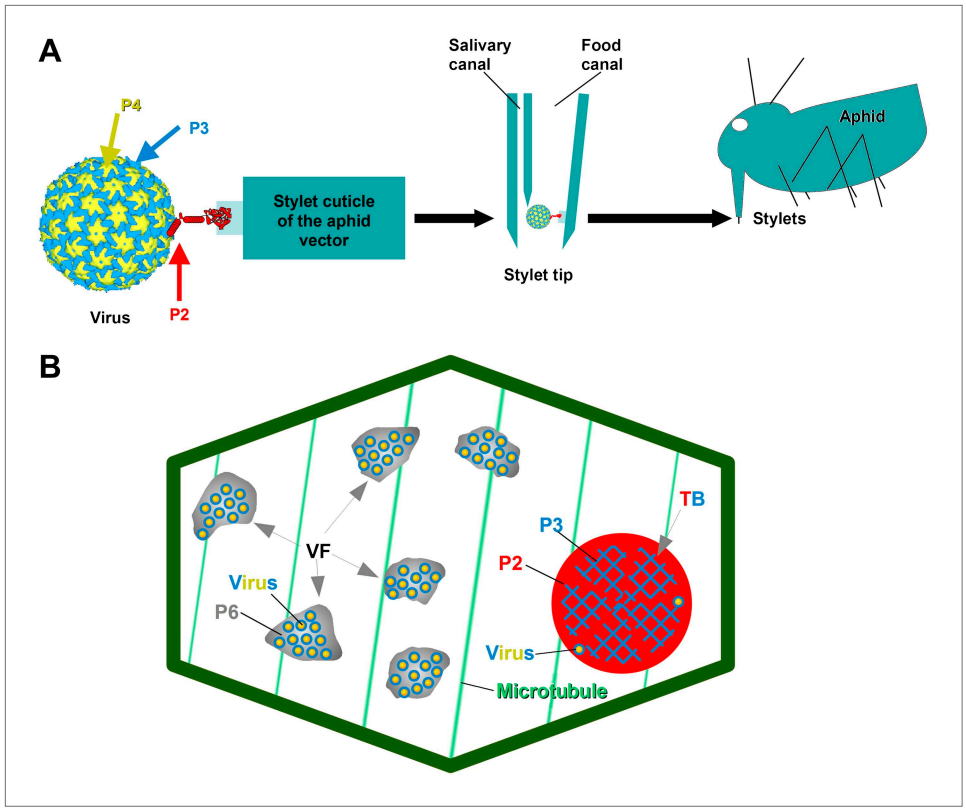

Figure 1. The CaMV transmissible complex and the transmission body. (**A**) Left: the CaMV transmissible complex comprises the virus particle, composed of capsid protein P4 (yellow), virus-associated protein P3 (blue) and the helper component P2 (red). P2 binds via its C-terminus to P3 and via its N-terminus to a protein receptor localized in the stylet tips of the aphid vector (middle and right). (**B**) Infected cells contain many cytoplasmic virus factories (VF), where most virus particles (blue-yellow circles) accumulate in a matrix composed of virus protein P6 (grey), and a single transmission body (TB). The TB (also cytoplasmic) is composed of P2 (red) and P3 (blue) as well as scattered virus particles. P3 in TBs is most likely in a conformation that differs from virus-associated P3. The spatial separation of the components of the transmissible complex (P2 in the TB and most virus particles in VFs) lead us to propose that they unite only at the moment of vector acquisition (***Drucker et al., 2002***). Cortical microtubules are designated in green and the cell wall in dark green. Cell organelles are not shown, for clarity. The CaMV model is from ***Plisson et al. (2005)***.

DOI: 10.7554/eLife.00183.003

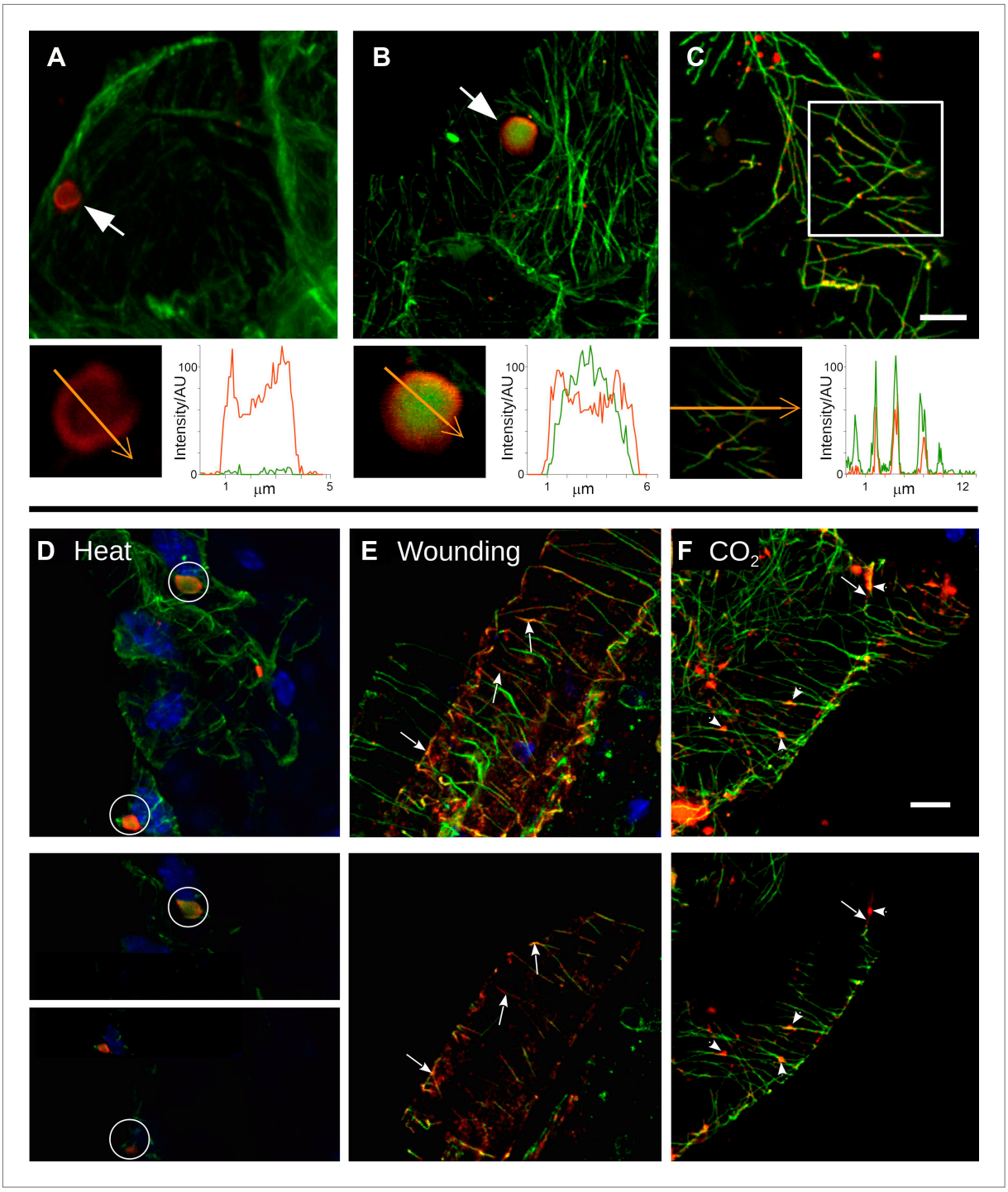

Figure 2. Stress induces different TB morphs. (**A**–**C**) The three TB morphs. Immunofluorescence of infected leaves against P2 (red) and α-tubulin (green), with co-labeling appearing as yellow/orange, reveals the different TB forms: (**A**) a tubulin-less TB (arrow), (**B**) a Tub$^+$|TB (arrow) and (**C**) mixed-networks. Images show confocal projections; insets show optical single sections from the TBs indicated by the arrows in (**A**) and (**B**), and of the enclosed zone in (**C**). The orange arrows in the insets mark the line scans and the direction used to create the profiles of P2 (red) and tubulin (green) label intensity, shown to the right of the insets. The line scans show that the TB in (**A**) contains hardly any tubulin, whereas the TB in (**B**) is heavily tubulin-labeled, revealing stronger tubulin labeling in the center of the TB than at the cortex. Finally, the distributions of P2 and tubulin labels colocalize in the mixed-networks shown in (**C**). The intensities are indicated in arbitrary units (AU) since the acquisition conditions were not identical for the different samples. (**D**–**F**) Stress induces TB transformation. Immunofluorescence labeling (P2 in red, tubulin in green, DAPI nucleic acid stain in blue) of infected leaves after the indicated stress treatment shows that heat shock (**D**) induces only Tub$^+$|TBs, whereas wounding stress (**E**) and exposure to CO_2 (**F**) additionally induce TB

Figure 2. Continued on next page

Figure 2. Continued

fragmentation (as revealed by the small red or orange foci in **E** and **F**) and mixed-networks. The upper panels of (**D**–**F**) show confocal projections, and the lower panels show selected optical single sections. For heat shock (**D**), two individual sections representing a median section through each of the two encircled TBs are shown. In (**E**–**F**), the arrows indicate filamentous P2 labeling that is continuous with microtubule labeling, and the arrowheads point to small P2 aggregates in the vicinity of microtubules. Scale bars: 5 μm. The confocal single sections used to create the projections shown here can be found in ***Figure 2—source data 1–6***. See also ***Figure 2—figure supplement 1*** that shows in vivo stress response of GFP-labeled tubulin in infected plants.

DOI: 10.7554/eLife.00183.004

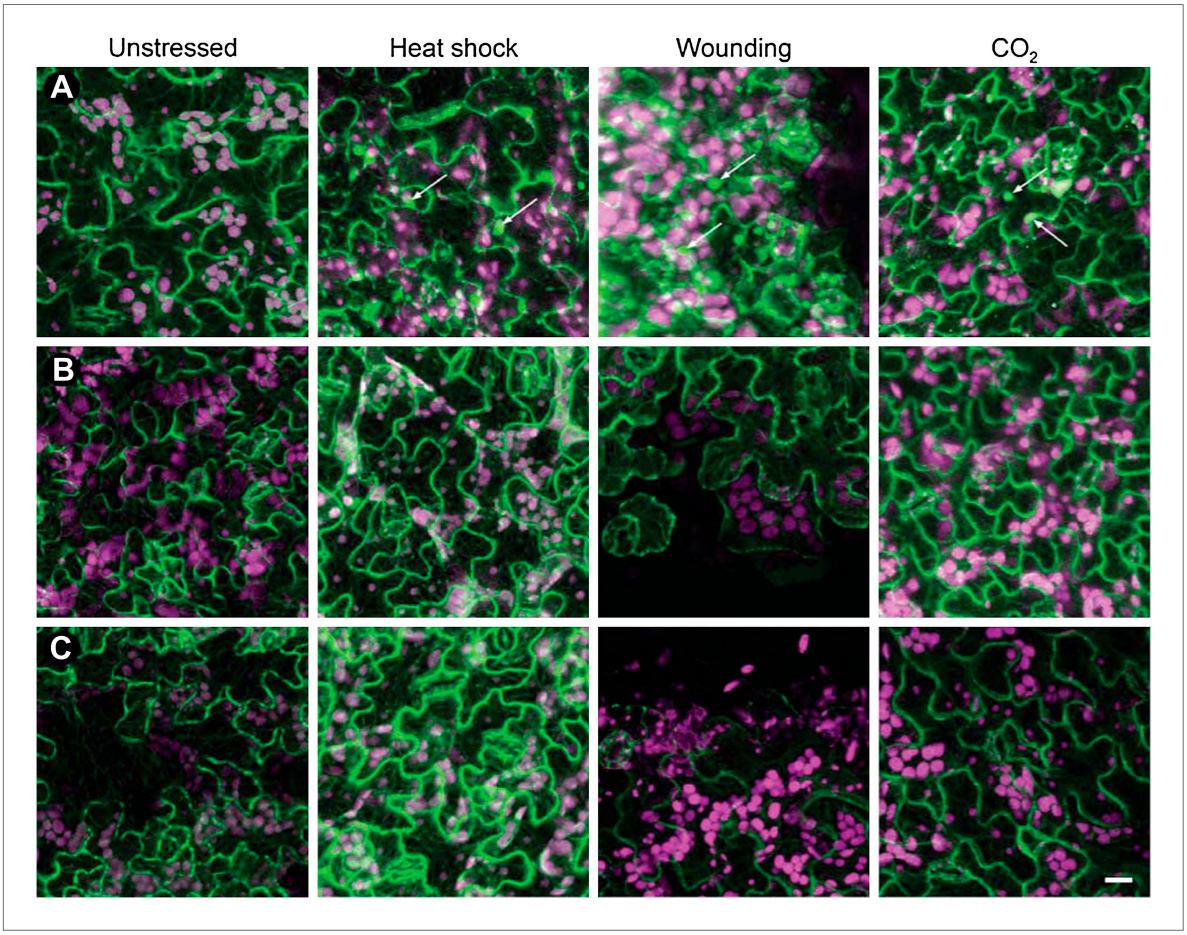

Figure 2—figure supplement 1. Tubulin accumulation in large inclusions after different stresses is specific to TBs. Confocal projections of Arabidopsis GFP-TUA6 leaves subjected to the stress indicated and examined by in vivo confocal fluorescence microscopy. (**A**) Wild type CaMV-infected leaf epidermis, (**B**) Leaf epidermis infected with the CaMV-ΔP2 mutant that does not form TBs, and (**C**) Healthy lead epidermis. Arrows indicate tubulin-containing TBs, visualized by live GFP-tubulin fluorescence (green). Chloroplast autofluorescence is shown in magenta. Note, however, that heat-shock induced some small GFP-tubulin aggregates. Scale bar = 10 μm.

DOI: 10.7554/eLife.00183.011

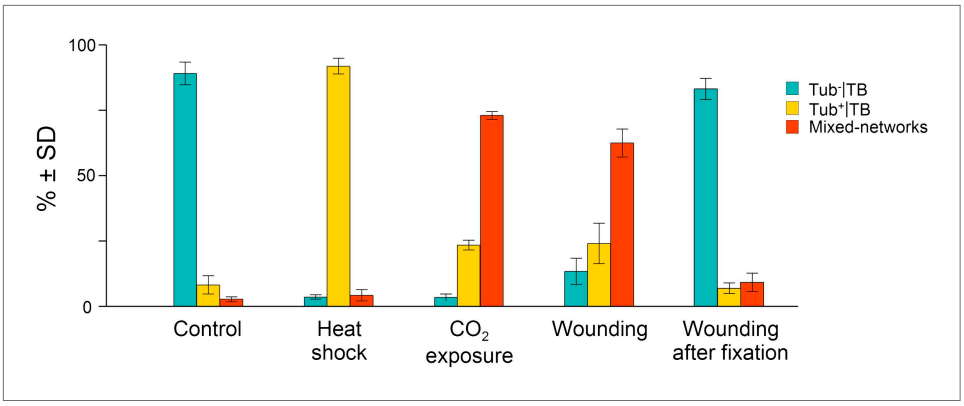

Figure 3. Quantitative analysis of the different TB morphs induced under stress conditions. Leaf samples were either left untreated (Control), exposed for 2 h at 37°C (Heat shock), exposed for 15 min to CO_2 atmosphere (CO_2 exposure), cut with a razor blade and then fixed within 10 s (Wounding), or fixed first and then cut with a razor blade (Wounding after fixation). All leaf samples were then processed in parallel for immunostaining against P2 and α-tubulin and scored for the occurrence of the different TB morphs: 'standby' Tub^-|TBs (turquoise), 'activated' Tub^+|TBs (yellow) or mixed-networks (red). Results are from three independent experiments and the total number of TBs and networks counted for each condition were control (284), heat shock (293), CO_2 exposure (282), wounding stress (313), and 288 in tissues wounded after fixation. See ***Figure 3—source data 1*** for details. SD: standard deviation.

DOI: 10.7554/eLife.00183.012

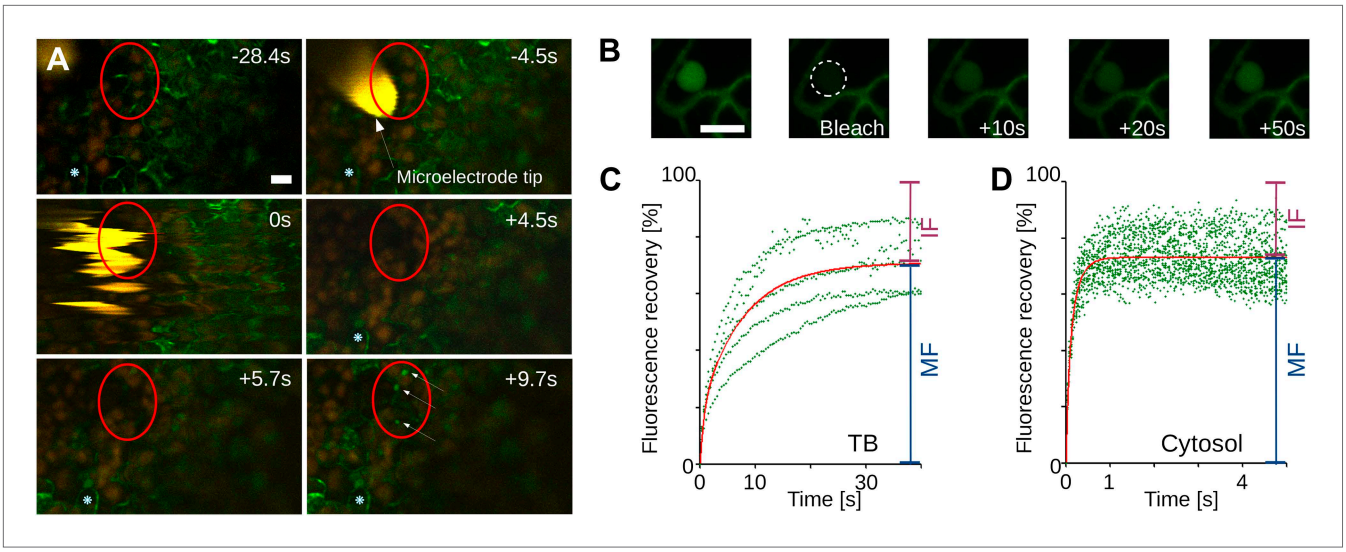

Figure 4. Tubulin influx into TBs occurs on a rapid time scale. (**A**) Kinetics of tubulin entry into TBs. The epidermis of CaMV-infected Arabidopsis leaves expressing GFP-tagged α-tubulin (Arabidopsis *GFP-TUA6*) was touched with a microelectrode tip (yellow), and the effect of the impact recorded by time-lapse confocal macroscopy. GFP-tubulin fluorescence is shown in green, chloroplast fluorescence in orange/red. Negative and positive time points are before and after the microelectrode-epidermis contact, respectively. The red circle denotes the impact zone, and the three arrows point to newly formed GFP-tubulin inclusions. The blue asterisk indicates a reference epidermis cell that did not change its z-position during the time lapse recording and can be used as a landmark for orientation. (**B**–**D**) Tubulin cycles between TBs and the cytoplasm. Arabidopsis *GFP-TUA6* plants were infected with CaMV and the epidermis was screened for rare spontaneously occurring Tub$^+$|TBs (no deliberate stress treatment was inflicted on the leaf); these were identified by the characteristic shape of the fluorescent tubulin-containing inclusions (see ***Figure 2—figure supplement 1***). The GFP-tubulin in these Tub$^+$|TBs was photobleached, and the recovery of the GFP fluorescence (due to replacement by fresh cytoplasmic GFP-tubulin) was recorded by time lapse microscopy. (**B**) Microscopic images of a typical FRAP experiment. The first picture shows a GFP-tubulin-containing Tub$^+$|TB before photobleaching. The dashed circle in the second picture indicates the photobleached zone at t = 0 s, and the following pictures show recovery of the GFP-fluorescence at indicated time points after photobleaching. (**C**–**D**) The graphs show quantifications of fluorescence recovery: after photobleaching of TBs (**C**), and after photobleaching of a cytoplasmic zone as a control of free tubulin diffusion (**D**). The fluorescence levels were normalized (100% = fluorescence before bleaching, 0% = fluorescence just after bleaching). For the two quantification graphs, FRAP trend lines (red) were calculated from seven FRAP experiments on GFP-tubulin-containing TBs, or from 18 FRAP experiments on cytoplasmic zones. The difference in $t_{(1/2)}$ for fluorescence recovery between TBs and the cytoplasm was highly significant ($p<0.0001$, t-test with n = 18 for TBs and n = 21 for cytoplasm). In contrast, the difference in the mobile fractions, that is, the percentage of exchangeable GFP-tubulin, the so-called mobile fraction, was not significant ($p=0.504$, t-test with n = 18 for TBs and n = 21 for cytoplasm). These results indicate that tubulin cycles between the cytoplasm and TBs, albeit at much slower rates than free diffusion in the cytoplasm. See ***Figure 4—source data 1 and 2*** for details. Scale bars: 10 μm; MF: mobile fraction; IF: immobile fraction.

DOI: 10.7554/eLife.00183.014

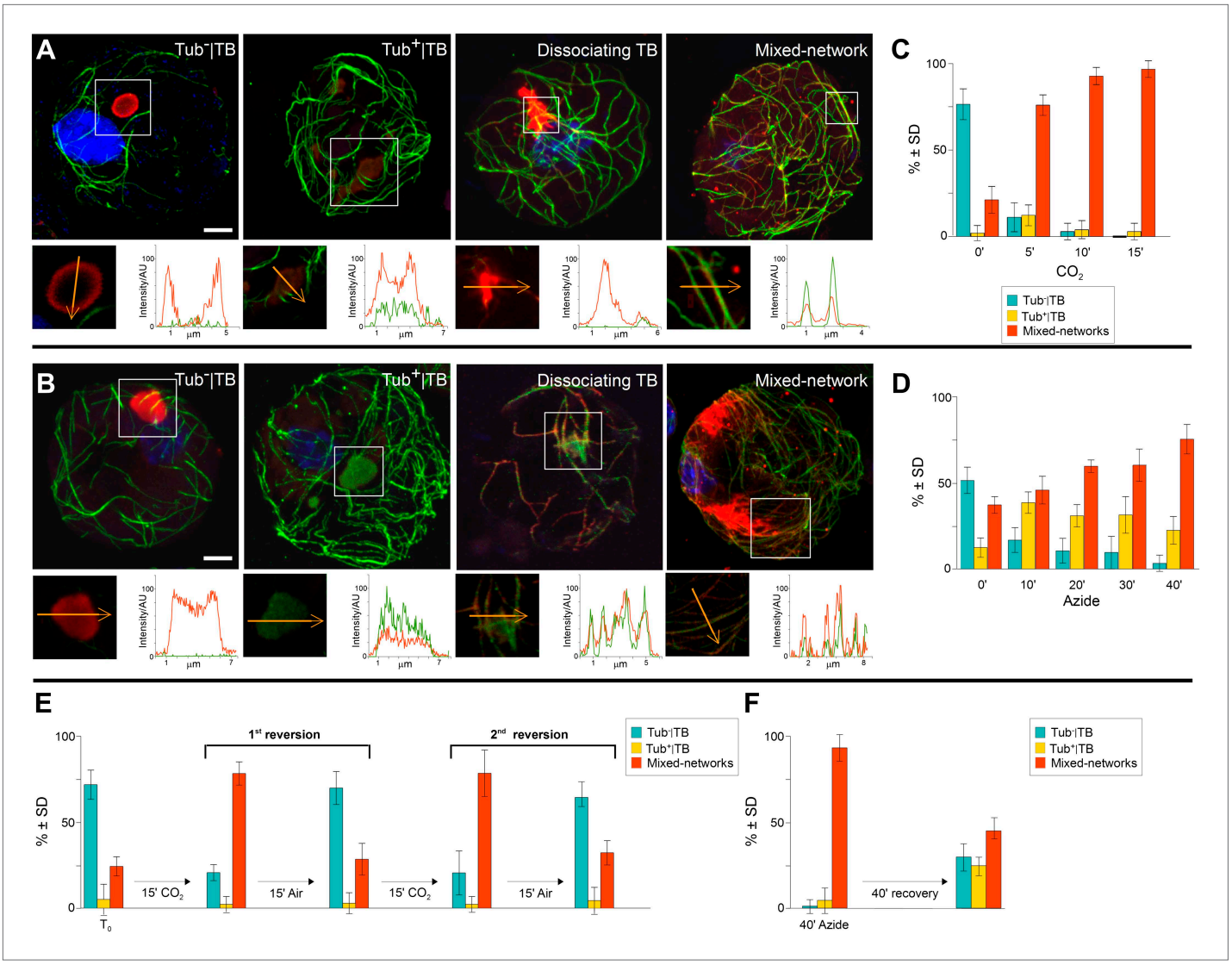

Figure 5. TB transformations have a precise temporal order and are reversible. (**A**–**B**) Kinetics of TB transformation. Protoplasts were treated with (**A**) CO_2 or (**B**) azide, and then processed for immunofluorescence against P2 (red) and α-tubulin (green); nuclei were counterstained with DAPI (blue). In both (**A**) and (**B**), untreated protoplasts display tubulin-less TBs, and the three subsequent images show representative treated protoplasts, respectively displaying a Tub⁺|TB, a disintegrating TB and mixed-networks. All images are confocal projections, with the exception of the dissociating TB after azide treatment, which is a single section; each inset shows a single optical section from the enclosed zone. The orange arrows show the line scans and the scanning direction used to create the profiles of P2 (red) and α-tubulin (green) labeling intensity (in arbitrary units, AU), which are displayed in the graphs to the right of the single sections. They reveal as in ***Figure 2A–C***, that unstressed TBs display little to no tubulin label, whereas stressed TBs contain large amounts of tubulin in their centers. P2 colocalizes with microtubules in mixed-networks. The confocal stacks used to generate the image projections can be found in ***Figure 5—source data 1 and 2***. (**C**–**D**) Quantification of TB kinetics. The histograms show the kinetics of CO_2- (**C**) and azide-triggered (**D**) TB transformation in protoplasts. Results from one out of three independent experiments are displayed. 1235 TBs (Tub⁻|TBs, Tub⁺|TBs, and mixed networks) were evaluated for the CO_2 experiments, and 1662 TBs were evaluated for the azide experiments. See ***Figure 5—source data 3 and 4*** for details. (**E**–**F**) Reversion of mixed-networks through two CO_2/air cycles (**E**), and after azide treatment (**F**). Infected protoplasts were treated with CO_2 or azide for the duration indicated. CO_2 was subsequently removed by ventilation of the suspension with air; azide was removed by resuspending the protoplasts in fresh medium. Shown are data from one of three independent experiments. For the three repetitions, a total of 1339 TB morphs were analyzed for CO_2 reversion, and 2262 TB morphs were analyzed for the azide reversion experiments. See ***Figure 5—source data 5 and 6*** for details. SD: standard deviation.

DOI: 10.7554/eLife.00183.020

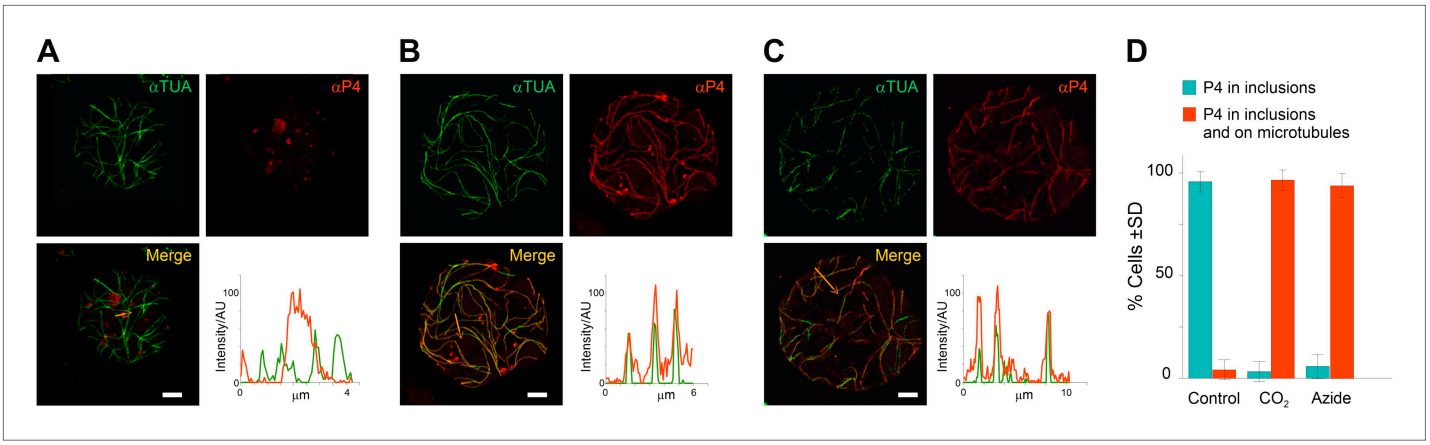

Figure 6. TB transformation mobilizes virus particles onto microtubules. (**A**–**C**) Viral capsid protein P4 colocalizes with mixed-networks. Protoplasts were either left unstressed (**A**), incubated with CO_2 for 15 min (**B**) or treated with azide for 40 min (**C**), and then fixed and labeled to detect capsid protein P4 (red) and α-tubulin (αTUA, green). The split channel representations and merges as well as the P4 and α-tubulin profiles obtained by scanning the lines indicated by the orange arrows show that the two stress treatments induced relocalization of capsid protein P4 from inclusions onto microtubules. As in ***Figure 2A–C***, the intensity of the P4 and α-tubulin label is indicated in arbitrary units (AU) because different acquisition settings were used to record the images. (**A**) is a confocal projection, (**B**–**C**) are confocal single sections. Refer to ***Figure 6—source data 1–3*** for image details. (**D**) Quantification of the effect of azide and CO_2 on the localization of P4. Cells were treated as indicated, processed for immunofluorescence against P4 and α-tubulin and scored for the presence of P4 in inclusions only, or in inclusions and on microtubules. The histogram shows that almost all cells display P4 networks that colocalize with microtubules after stress treatment. Data are from one of three independent experiments, in which a total of 524 cells were analyzed. Refer to ***Figure 6—source data 4*** for details. Scale bars: 5 µm. SD: standard deviation.

DOI: 10.7554/eLife.00183.027

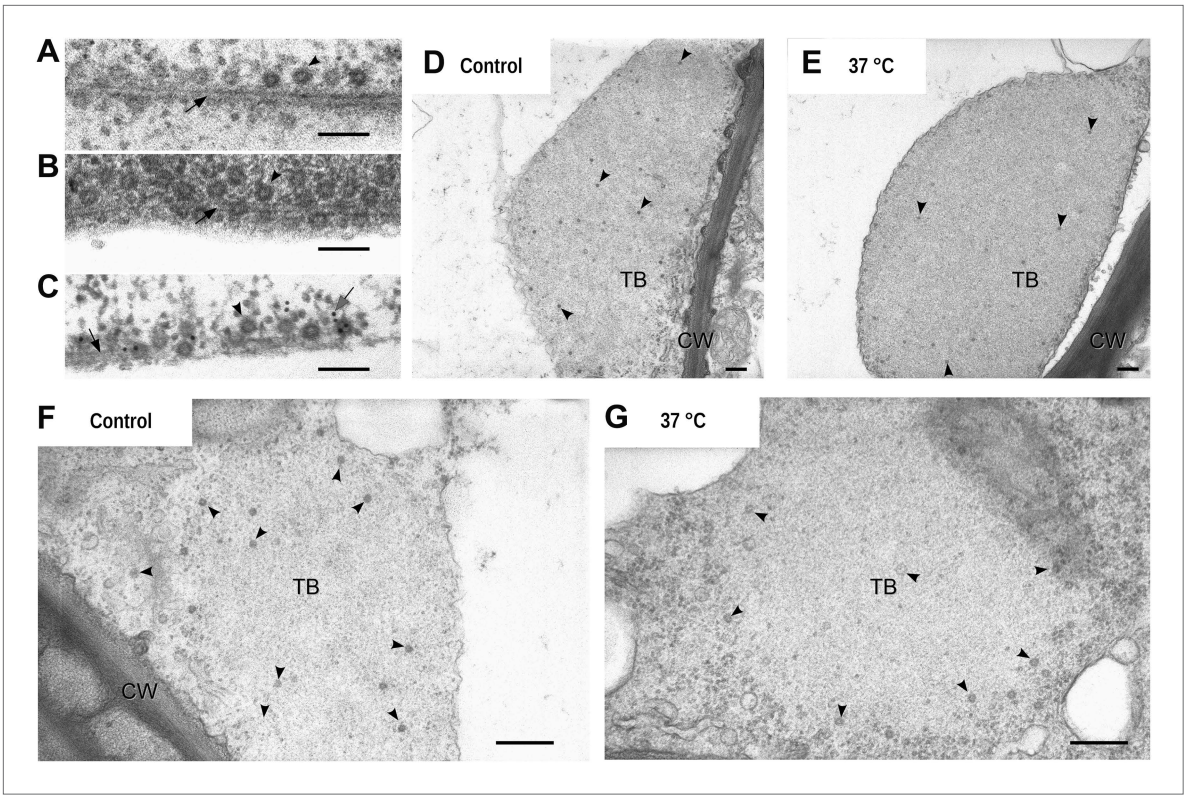

Figure 7. Electron microscopy of the different TB morphs. (**A**–**C**) Mixed-networks display virus particles on microtubules. The images show typical spherical CaMV virus particles (arrowheads) that decorate microtubules (black arrows) in cortical regions of (**A**) a CO_2-treated or (**B**) an azide-treated protoplast. (**C**) Positive immunogold labeling against P2 (the gray arrow points to an exemplary nanogold particle) identifies the virus-decorated microtubules as mixed-networks, in which all components of the CaMV transmissible complex are present. (**D**–**G**) TBs in unstressed (**D**, **F**) and heat-shocked (**E**, **G**) tissue display the same TB phenotype. Infected Arabidopsis *TUA6-GFP* leaves were exposed for 1 h at 37°C. The presence of tubulin in TBs was then verified by fluorescence microscopy and the same leaf samples were processed for transmission electron microscopy. The arrowheads point to virus particles. CW: cell wall. For scale bars, (**A**–**C**): 100 nm; (**E**–**G**): 250 nm.

DOI: 10.7554/eLife.00183.032

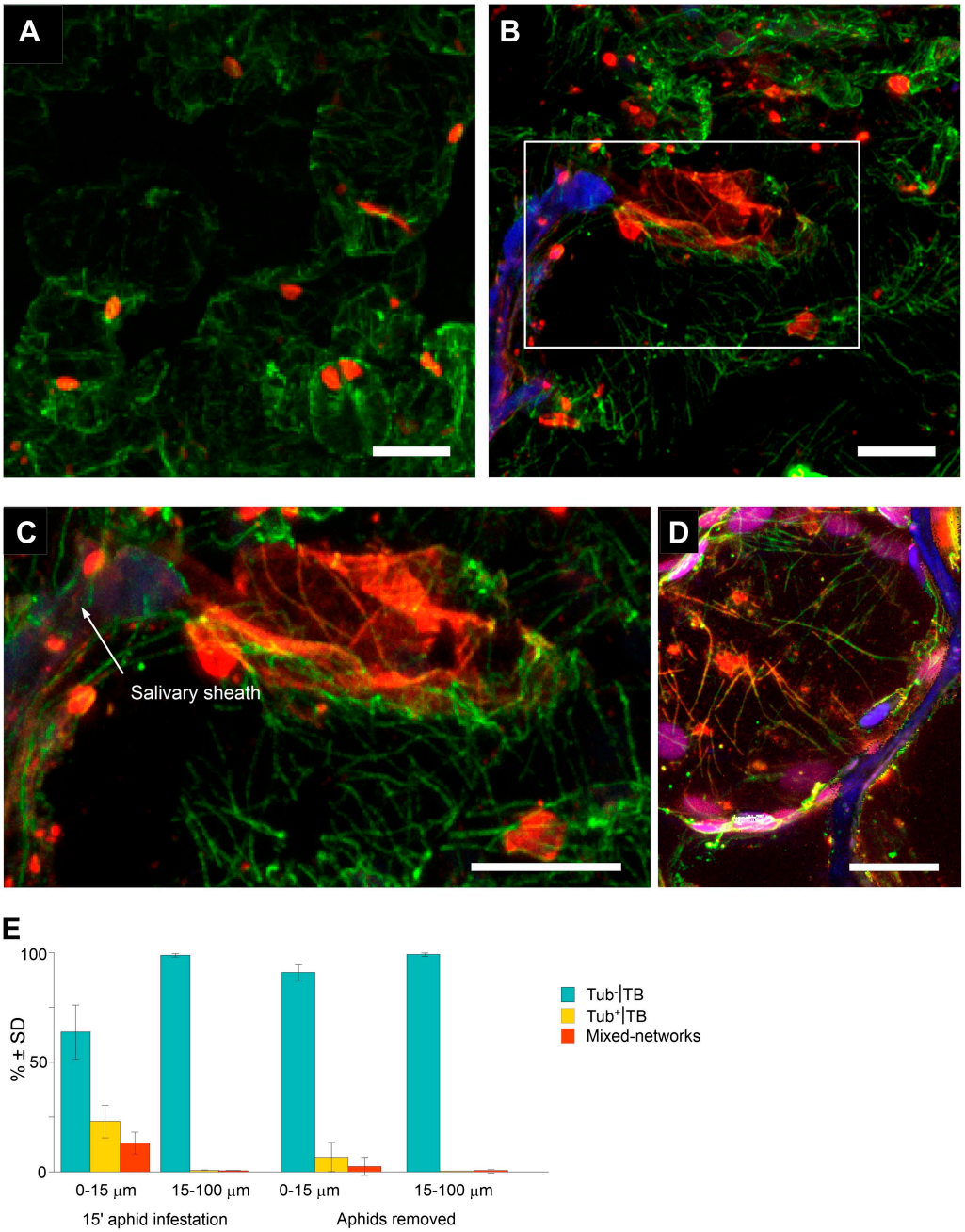

Figure 8. Mixed-networks appear in tissue zones pierced by aphid stylets. Unstressed CaMV-infected leaves (**A**) or leaves infested by aphids for 15 min (**B**–**D**) were analyzed by immunofluorescence microscopy. (**A**) Cells in leaf regions that were not foraged by aphids display standby Tub⁻|TBs, as shown by confocal projections of tissue sections labeled against P2 (red) and α-tubulin (green). The optical single sections used for this projection are deposited in ***Figure 8—source data 1***. (**B**) In contrast, a cell close to a salivary sheath (blue autofluorescence, digitally enhanced) displays mixed-networks, in aphid-infested tissue. An enlargement of the zone enclosed in (**B**) is shown in (**C**). (**B**–**C**) show confocal projections, please refer to ***Figure 8—source data 2*** for the corresponding image stack. (**D**) Immunofluorescence microscopy against capsid protein P4 (red) and α-tubulin (green) shows that virus particles also localize to mixed-networks in cells close to salivary sheaths (blue, digitally enhanced). Chloroplast autofluorescence appears in magenta. The confocal single sections used to produce this projection can be found in ***Figure 8—source data 3***. (**E**) Aphids trigger TB transformation, and this transformation is

Figure 8. Continued on next page

Figure 8. Continued

reversible. Aphids were placed for 15 min on infected leaves. Following this, the leaves were fixed immediately and processed for immunofluorescence (15-min aphid infestation), or the aphids were removed and the leaves were processed 2 h later (Aphids removed). The TB phenotype (standby Tub^-|TBs, Tub^+|TBs and mixed-networks) was scored next to salivary sheaths (0–15 μm) and in surrounding tissue (15–100 μm). Tub^+|TBs and mixed-networks were predominantly observed close to salivary sheaths in freshly aphid-infested tissue. The effect was highly significant ($p<0.0001$, GLM, df = 1, $\chi^2 = 194.59$, n = 3). Tub^+|TBs and mixed-networks reverted back to 'stand-by' Tub^-|TBs 2 h after aphid removal, indicating that TB activation is reversible. This effect was also highly significant ($p<0.0001$, GLM, df = 1, $\chi^2 = 17.98$, n = 3). SD in (**E**): standard deviation from three independent experiments. A total of 969 TBs surrounding 42 sheaths were counted from freshly aphid-infested tissue, and 194 TBs surrounding eight sheaths were counted in the 'aphids removed' experiments. Original data can be found in ***Figure 8—source data 4***.

DOI: 10.7554/eLife.00183.033

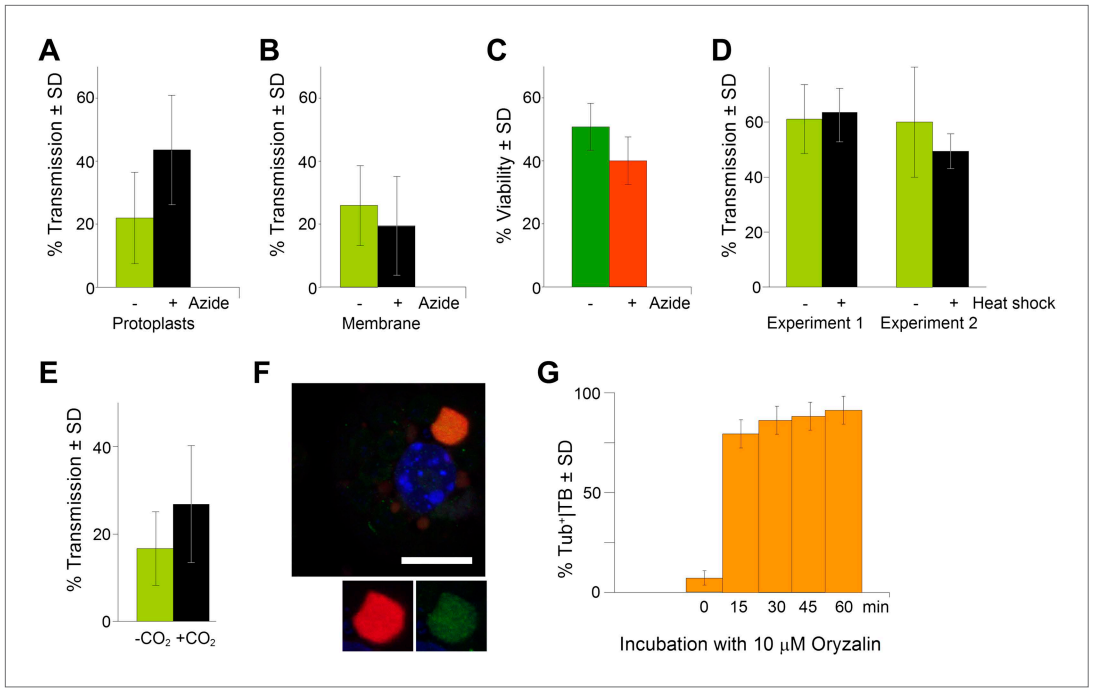

Figure 9. TB transformation correlates with enhanced transmission efficiency. (**A**) Azide enhances transmission from protoplasts. Aphids were allowed to acquire CaMV from infected protoplasts that displayed mixed-networks induced by azide. They were then transferred to healthy test plants for inoculation, and infected plants were counted 3 weeks later. The difference in transmission was highly significant ($p<0.0001$, hierarchical GLM model, ***Table 3*** and ***Figure 9—source data 1***). (**B**) Azide does not affect aphid behavior. To rule out an unwanted effect of azide on aphid viability and behavior, aphids were membrane-fed solutions containing purified virus particles, recombinant P2 and P3, in the presence or absence of azide, and then transferred to healthy test plants for inoculation. Transmission rates were determined 3 weeks later by scoring infected plants. Data from one experiment are shown, using three different virus preparations as a virus source for each condition. See ***Figure 9—source data 2*** for details. (**C**) Azide does not affect protoplast viability. Protoplasts were incubated for 1 h (the duration of a transmission test) in the presence or absence of 0.02% azide, and then protoplast viability was determined with the FDA test (***Widholm, 1972***). Data from one out of two experiments are shown. The difference in viability was insignificant in this experiment ($p=0.0658$, $n = 6$, Mann–Whitney test) and also in the second experiment. See ***Figure 9—source data 3*** for all data. (**D**) Heat shock does not enhance CaMV transmission. Leaves from *GFP-TUA6* Arabidopsis either received heat shock (+) or did not (−). The presence of Tub^+|TBs was verified by fluorescence microscopy and the leaves were then used in aphid transmission assays. No significant difference in transmission was observed in either of two independent experiments ($p=0.73$ and $p=0.08$, respectively, hierarchical GLM model, see ***Table 4*** and ***Figure 9—source data 4***). (**E**) CO_2 enhances CaMV transmission. Leaves with mixed-networks induced by CO_2 were used in plant-to-plant aphid transmission experiments. CO_2-treated leaves performed significantly better in transmission tests than controls ($p=0.0025$, hierarchical GLM model, see ***Table 5*** and ***Figure 9—source data 5***). (**F**) Oryzalin induces Tub^+|TBs. Immunofluorescence of oryzalin-treated protoplasts shows that α-tubulin (green) accumulates with P2 (red) in TBs. The nucleus is stained with DAPI (blue). The image is a confocal projection. The insets show a separate channel presentation of a representative optical single section of the TB, for details refer to the image stack in ***Figure 9—source data 6*** that was used for this projection. Scale bar = 10 μm. (**G**) Kinetics of Tub^+|TB formation in protoplasts that were treated with oryzalin for the duration indicated. Most TBs transformed to the Tub^+-state within 15 min. Mixed-networks were not observed and thus are not indicated in the histogram. Data is from one of three independent experiments, where a total of 1556 TBs were analyzed. See ***Figure 9—source data 7*** for details. SD: standard deviation.

DOI: 10.7554/eLife.00183.038

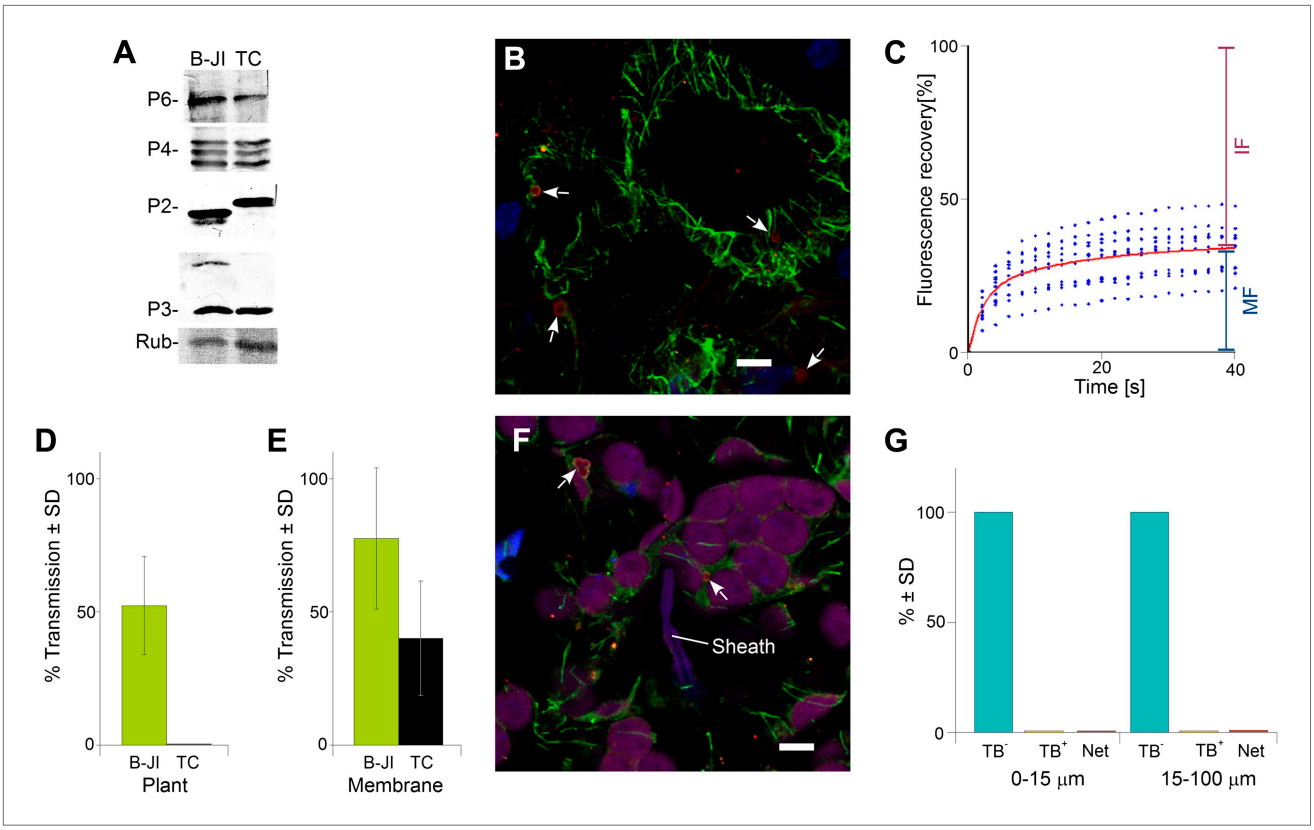

Figure 10. The P2-TC mutant of CaMV is inactive in plant-to-plant transmission. (**A**) Accumulation of viral proteins in CaMV P2-TC-infected plants. Western blot analysis of total leaf extracts shows that virus factory protein P6, the three forms of capsid protein P4, as well as P2 and P3 accumulate to similar levels in plants infected with wild type CaMV (B-JI) or the P2-TC mutant (TC). Rub = Rubisco loading control stained with Ponceau Red. (**B**) CaMV P2-TC-infected plants display TBs. Confocal projection of infected leaf sections labeled for P2 (red) and α-tubulin (green) shows that the CaMV mutant P2-TC forms TBs (arrows) that are smaller and more regular than wild type TBs. Nuclei are counterstained with DAPI (blue). The optical single sections used for the projection are presented in ***Figure 10—source data 1***. (**C**) Tubulin turnover in P2-TC mutant TBs. Arabidopsis plants constitutively expressing GFP-tubulin were infected with the CaMV P2-TC mutant. Leaf epidermis was screened by fluorescence microscopy for GFP-tubulin inclusions that were identified as TBs based on their typical shape. The GFP-tubulin was photobleached in these TBs, and the recovery of the GFP-fluorescence (due to replacement of the photobleached GFP-tubulin by fresh tubulin) was recorded in FRAP experiments. The graph shows recovery kinetics from t = 0 s (time point of photobleach) onwards. The fluorescence levels were normalized (100% = fluorescence before bleaching, 0% = fluorescence just after bleaching). The red trend line was calculated from nine experiments. Data points from the nine experiments are indicated as blue dots. These results indicate that tubulin cycles between the cytoplasm and mutant TBs, albeit with different kinetics than for wild type TBs (compare with ***Figure 4C***). Compared to wild type TBs, the $t_{(1/2)}$ for fluorescence recovery was significantly slower ($p<0.0001$, t-test with n = 21 for wild type TBs and n = 23 for TC-TBs) and the proportion of the mobile fraction was significantly higher in P2-TC TBs ($p=0.0001$, t-test with n = 21 for wild type TBs and n = 23 for TC-TBs). Refer to ***Figure 10—source data 2*** and ***Figure 4—source data 1*** (wild type TBs) for data sets. (**D**) The mutant P2-TC does not support plant-to-plant transmission. Aphids were placed for 15 min on CaMV wild type-infected (B-JI) or P2-TC-infected (TC) leaves and then transferred to healthy test plants for inoculation. Infected plants were scored 3 weeks later. Pooled data are shown from two independent experiments using 12 different leaves for each condition. No statistical analysis was performed, as the effect of the P2-TC mutant on plant-to-plant transmission was total (no transmission from P2-TC-infected plants was observed). See ***Figure 10—source data 3*** for the data sets. (**E**) The P2-TC protein itself is active in transmission. Recombinant wild type P2 (B-JI) or mutant P2-TC (TC) were mixed together with recombinant P3 protein and purified CaMV particles. Aphids were allowed to feed on the suspensions across membranes for 15 min and were then transferred to healthy test plants for inoculation. Infected plants were counted 3 weeks later. The histogram shows that P2-TC supported aphid transmission of CaMV under these conditions, although this was significantly reduced as compared to the wild type P2 ($p=0.02$, n = 8 from two independent experiments, Mann–Whitney test). See ***Figure 10—source data 4*** for data. (**F**) Aphid stylet activity does not trigger TB transformation in CaMV P2-TC-infected leaves. Aphids were allowed to feed on CaMV-P2-TC-infected leaves for 15 min. The tissue was then processed for immunofluorescence against P2 (red) and α-tubulin (green); nuclei were stained with DAPI (blue). The confocal projection in (**F**) indicates that cells in contact with a salivary sheath (Sheath) display tubulin-less TBs (arrows). Chloroplasts are displayed in magenta to better distinguish the cells. Please see ***Figure 10—source data 5*** for the confocal single sections used to create the projection. (**G**) Quantitative analysis of the TB forms of CaMV-P2-TC in aphid-infested tissue reveals the absence of Tub^{+}|TBs and mixed-networks, both close to salivary sheaths (0–15 µm) and farther away (15–100 µm). Data shown are from three independent experiments where a total of 510 TBs were analyzed (see ***Figure 10—source data 6*** for details). As the effect was total, no statistical analysis was performed. SD: standard deviation.
DOI: 10.7554/eLife.00183.049

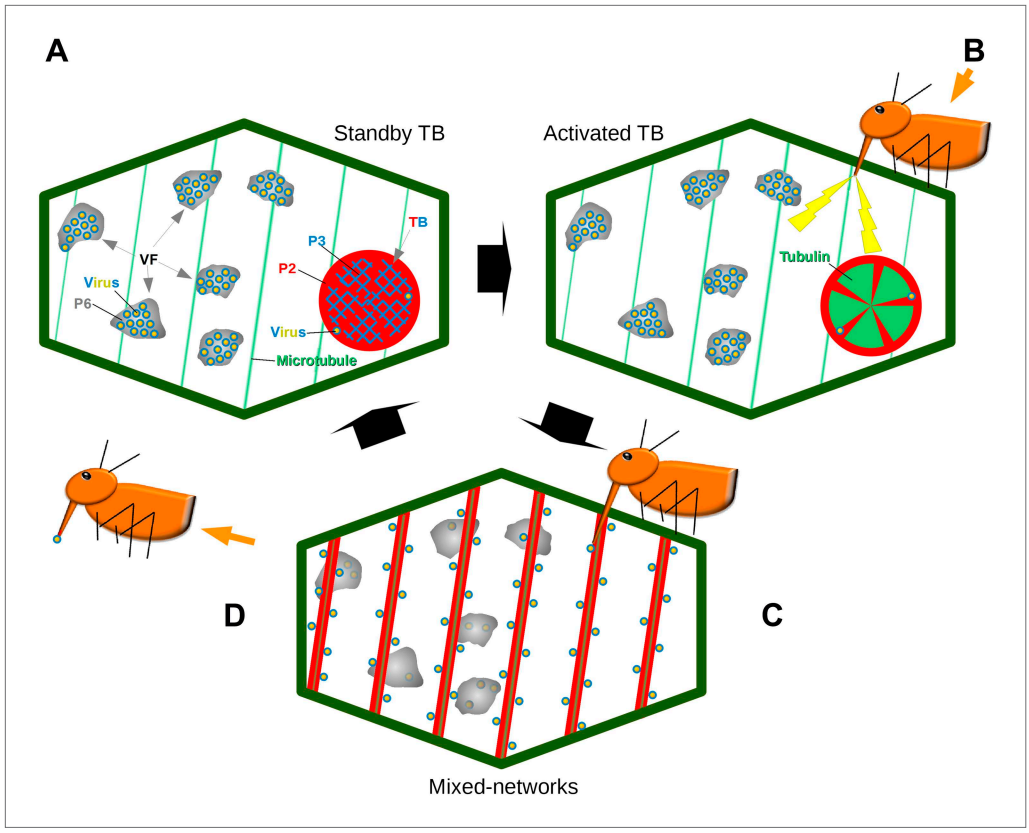

Figure 11. Model of CaMV acquisition. (**A**) In an infected cell in the 'standby' state, there are numerous virus factories (VF) containing most of the replicated virus particles (yellow-blue circles), enclosed within a matrix of viral protein P6 (grey). This is accompanied in the cell by a mostly single transmission body (TB), composed of a matrix containing all of the cell's P2 (red), co-aggregated with P3 (blue) and some virus particles. Microtubules are represented in green. (**B**) An aphid landing on an infected plant inserts its stylets into a cell to test the plant. This causes a mechanical stress (stylet movement) and/or a chemical stress (e.g., elicited by saliva components). This stress, symbolized by the yellow flashes, is immediately perceived by the plant and can induce subsequent defense responses. The initial aphid recognition signal is transduced simultaneously in a TB response, characterized by an influx of tubulin (green) into the TB. (**C**) In a second step, the TB disintegrates rapidly (within seconds), and all the P2 as well as some virus particles relocalize on the cortical microtubules as mixed-networks. Whether or not the virus particles originate at the VFs, as presented here, is unknown. Transmissible P2-virus complexes are now homogeneously distributed throughout the cell periphery, which significantly increases the chances of successful binding of P2 and virus to the stylets and thus transmission. (**D**) After departure of the aphid vector (here loaded with P2 and virus), a new TB is reformed from the mixed-networks and is ready for another round of transmission.
DOI: 10.7554/eLife.00183.056